Truncation of Limonene Synthase Preprotein Provides a Fully Active 'Pseudomature' Form of This Monoterpene Cyclase and Reveals the Function of the Amino-Terminal Arginine Pair†

David C. Williams, Douglas J. McGarvey,‡ Eva J. Katahira, and Rodney Croteau*

Institute of Biological Chemistry, and Department of Biochemistry and Biophysics, Washington State University, Pullman, Washington 99164-6340

Received April 16, 1998; Revised Manuscript Received June 25, 1998

ABSTRACT: The monoterpene cyclase limonene synthase transforms geranyl diphosphate to a monocyclic olefin and constitutes the simplest model for terpenoid cyclase catalysis. (−)-4*S*-Limonene synthase preprotein from spearmint bears a long plastidial targeting sequence. Difficulty expressing the full-length preprotein in *Escherichia coli* is encountered because of host codon usage, inclusion body formation, and the tight association of bacterial chaperones with the transit peptide. The purified preprotein is also kinetically impaired relative to the mixture of N-blocked native proteins produced in vivo by proteolytic processing in plastids. Therefore, the targeting sequence, that precedes a tandem pair of arginines (R58R59) which is highly conserved in the monoterpene synthases, was removed. Expression of this truncated protein, from a vector that encodes a tRNA for two rare arginine codons (pSBET), affords a soluble, tractable 'pseudomature' form of the enzyme that is catalytically more efficient than the native species. Truncation up to and including R58, or substitution of R59, yields enzymes that are incapable of converting the natural substrate geranyl diphosphate, via the enzymatically formed tertiary allylic isomer 3*S*-linalyl diphosphate, to (−)-limonene. However, these enzymes are able to cyclize exogenously supplied 3*S*-linalyl diphosphate to the olefinic product. This result indicates a role for the tandem arginines in the unique diphosphate migration step accompanying formation of the intermediate 3*S*-linalyl diphosphate and preceding the final cyclization reaction catalyzed by the monoterpene synthases. The structural basis for this coupled isomerization−cyclization reaction sequence can be inferred by homology modeling of (−)-4*S*-limonene synthase based on the three-dimensional structure of the sesquiterpene cyclase epi-aristolochene synthase [Starks, C. M., Back, K., Chappell, J., and Noel, J. P. (1997) *Science 277*, 1815−1820].

The terpenoids comprise the largest family of natural products; some 20 000 structures have now been defined (*1*), a number that exceeds the alkaloids and phenylpropanoids combined (*2*). All of the lower terpenoids are derived via the polymerization of isopentenyl diphosphate by prenyltransferases that catalyze formation of the C_{10} (geranyl), C_{15} (farnesyl), and C_{20} (geranylgeranyl) acyclic prenyl diphosphate intermediates (*3*) which are then cyclized to the various monoterpene, sesquiterpene, and diterpene carbon skeletons, respectively, by the corresponding terpene synthases [*4*, *5*; for recent comprehensive reviews, see Cane (*6*)]. These enzymes have received considerable recent attention because the cyclization process determines the basic structural character of the terpenoid end products and because the electrophilic cyclization mechanisms are quite complex, involving multiple steps in which many of the carbon atoms of the substrate undergo alterations in bonding, hybridization, and configuration (*7*, *8*).

Scheme 1: Isomerization and Cyclization of Geranyl Diphosphate to (−)-Limonene, via 3*S*-Linalyl Diphosphate and the 4*S*-α-Terpinyl Cation, and Subsequent Redox Conversion of the Olefin to (−)-Menthol and (−)-Carvone

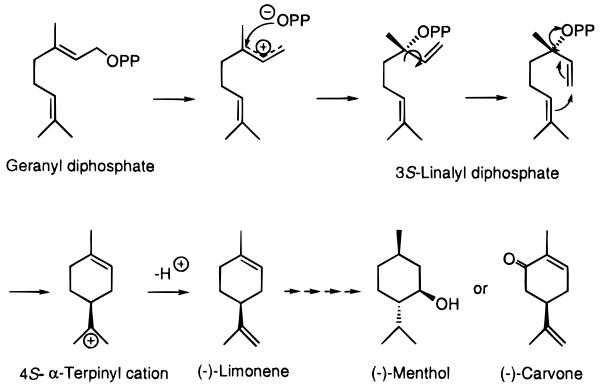

(−)-4*S*-Limonene synthase catalyzes the divalent metal ion-dependent conversion of geranyl diphosphate, via bound (+)-3*S*-linalyl diphosphate, to the monocyclic monoterpene olefin (*9*) (Scheme 1). This transformation constitutes one of the simplest of all terpenoid cyclization reactions (*10*) and

† D.C.W. and D.J.M. share equal credit in this investigation which was supported by National Institutes of Health Grant GM 31354, by Project 0268 from the Washington State University Agricultural Research Center, and by the WSU Plant Biochemistry Research and Training Center (DOE DE-FG06-94ER20160).

* To whom correspondence should be addressed. Phone: (509) 335-1790. Fax: (509) 335-7643. E-mail: croteau@mail.wsu.edu.

‡ Present address: QIAGEN GmbH, Max-Volmer-Strasse 4, D-40724 Hilden, Germany.

S0006-2960(98)00854-X CCC: $15.00
Published on Web 08/14/1998

has ample precedent in biomimetic solvolysis studies (*11*−*13*), and, thus, limonene synthase has become a model for this class of enzymes (for review, see *8*). Limonene synthase was first isolated from mint (*Mentha*) species, where it catalyzes the dedicated step in the biosynthesis of the characteristic components of the essential oils [i.e., (−)-menthol in peppermint (*Mentha* x *piperita*) and (−)-carvone in spearmint (*Mentha spicata*) (Scheme 1)], and it was shown to be a typical terpene synthase in properties and reaction mechanism (*9*, *14*). Limonene has been implicated recently as a dietary anticarcinogen (*15*).

A reverse genetic approach was utilized to isolate the limonene synthase cDNA from a spearmint leaf library, and the recombinant synthase was shown to produce the same olefin mixture as the native enzyme [94% (−)-limonene with about 2% each of myrcene, (−)-α-pinene, and (−)-β-pinene] by functional expression of the preprotein in *Escherichia coli* (*16*). The cDNA is 1800 nucleotides in length and encodes a 72.4 kDa protein bearing a substantial amino-terminal plastidial targeting peptide; in planta, the preprotein is imported into the plastids where it is proteolytically processed to the mature form(s) of about 65 kDa.[1]

To obtain sufficient amounts of limonene synthase for detailed mechanistic and structural study, high-level expression of the catalytically competent enzyme is required. However, heterologous overexpression of the preprotein in *E. coli* proved to be problematic. The bacterially expressed preprotein tends to form intractable inclusion bodies, and the soluble species, even when expressed as $(his)_6$•tagged or glutathione-*S*-transferase fusions, is difficult to purify, as binding to the corresponding metal ion chelation or glutathione-affinity columns is adversely influenced by associated *E. coli* chaperones, which apparently copurify with the synthase. The expressed preprotein, when purified in sufficient amounts for kinetic characterization, is compromised in both K_m and k_{cat} relative to the native species.

These serious shortcomings were attributed to the presence of the large plastidial transit peptide, the precise size of which could not be directly determined. The native enzyme is N-terminally blocked and is not apparently deblocked by deglycosylation, deacylation, or pyroglutamase treatment, thereby preventing determination of the transit peptide−mature protein junction by amino-terminal sequencing. Electrospray mass spectrometric analysis of the purified native enzyme indicated that this protein exists as a heterogeneous population of modified forms. In vitro translation of the cDNA in the presence of multiple, radiolabeled amino acids, followed by import and processing in isolated pea chloroplasts, and radiochemically based sequencing of the resulting mature protein, also gave ambiguous results suggesting imprecise proteolytic cleavage.[1] Finally, predictive methods for defining the two most probable cleavage sites (*17*, *18*) gave, when the corresponding cDNA truncations were constructed and expressed, proteins that were inactive and shown to be too short by SDS−PAGE comparison to the native enzyme from spearmint.

It was apparent that systematic truncation and testing of the resulting expressed proteins would be required in order to prepare a limonene synthase suitable for detailed study. In this paper, we report the construction and kinetic evaluation of a series of truncated forms of the preprotein, describe the preparation of a highly active and tractable 'pseudomature' form of limonene synthase, and discuss the implications of these findings for monoterpene cyclase active site structure and function.

EXPERIMENTAL PROCEDURES

Materials and General Procedures. [1-^{3}H]Geranyl diphosphate (120 Ci/mol) was prepared as previously described (*19*), as was 3*S*-[1*Z*-^{3}H]linalyl diphosphate (38.2 Ci/mol) (*20*). The typical assay for (−)-4*S*-limonene synthase employed 1−50 μg of native or recombinant protein in 25 mM MOPSO[2] buffer (pH 7.0) containing 15 mM $MgCl_2$, 1.0 mM DTT, and 25 μM geranyl diphosphate. All samples were changed to these buffer conditions by dilution, dialysis, or desalting (Econo-Pac 10DG desalting column, Bio-Rad) prior to assay by solvent extraction and chromatographic isolation of the olefinic product as described previously (*14*). The identity of the product (94% limonene with roughly 2% each of myrcene, α-pinene and β-pinene) was confirmed by combined GLC-(EI)MS,[2] as previously described (*9*, *16*) using terpenoid standards from our own collection. For the determination of kinetic constants, triplicate assays were conducted (at a minimum of 10 substrate concentrations ranging from 0.2 to 180 μM geranyl diphosphate or 3*S*-linalyl diphosphate, at saturating levels of the required divalent metal ion cofactor), and control incubations (without enzyme) were included in all cases to adjust for background due to increasing substrate concentration. A double reciprocal plot was generated for each averaged data set, and the equation of the best-fit line ($r > 0.95$) was determined (KaleidaGraph, version 3.08, Synergy Software, Reading, PA). Limonene synthase does not exhibit simple kinetics typical of monomeric enzymes. At low substrate concentrations (up to 30 μM), velocity increases hyperbolically, and then shows an inflection between 30 and 40 μM before reaching saturation. Since the substrate concentration in vivo is expected to be less than 10 μM [geranyl diphosphate cannot be detected in vivo, even by saturation $^{14}CO_2$ labeling (*21*)], this unusual behavior at higher substrate concentrations is not likely to be physiologically relevant. Kinetic parameters were established from response curves in the 1−40 μM substrate concentration range, consistent with previous studies with this enzyme (*9*, *14*, *22*). Protein concentrations were determined by the modified method of Bradford (*23*) using the Bio-Rad BCA assay with purified limonene synthase [expressed from pSBETaLC(R58)8-8; see below] as standard, or directly by UV absorption (A_{280}) using the calculated extinction coefficient $\epsilon_{280} = 109\,400\ M^{-1}\ cm^{-1}$. The olefin mixture produced by the enzyme at both low and high substrate concentrations was verified by GC-MS as above.

SDS−PAGE was performed according to Laemmli (*24*), and the protein bands and molecular weight markers were

[1] J. Gershenzon, G. Turner, E. Nielsen, and R. Croteau, in preparation.

[2] Abbreviations: bp, base pair(s); DTT, dithiothreitol; EI, electron impact; ES, electrospray; GLC, gas-liquid chromatography; HPLC, high-performance liquid chromatography; LSC, liquid scintillation counting; MS, mass spectrometry; MOPSO, 3-(*N*-morpholino)-2-hydroxypropanesulfonic acid; nt, nucleotide(s); PAGE, polyacrylamide gel electrophoresis; PCR, polymerase chain reaction; SDS, sodium dodecyl sulfate.

located by Coomassie Brilliant Blue R-250 (*14*) and silver staining (*25*). When necessary to estimate the purity of protein samples which could not be brought to homogeneity, Coomassie and silver-stained gels were evaluated by laser densitometry (*16*). Monospecific, polyclonal antibody preparation, using native limonene synthase from spearmint as antigen, and procedures for immunoblotting have been described elsewhere (*26*).

PCR was performed in volumes of 100 μL containing 20 mM Tris-HCl (pH 8.8), 10 mM KCl, 10 mM $(NH_4)_2SO_4$, 2 mM $MgCl_2$, 0.1% Triton X-100, 5 μg of bovine serum albumin, 200 μM each dNTP, 0.2 μM each primer, 3.7 units of recombinant *Pfu* DNA polymerase (Stratagene), and 25 ng of linearized template DNA, at 95 °C for 1 min, 52 °C for 1 min, and 72 °C for 3.5 min, for 30 cycles followed by a 10 min final extension period at 72 °C. The conditions were modified only slightly (pH 9.0, 50 mM KCl, 1.0 μM of each primer) when *Taq* DNA polymerase (2.5 units) was employed. The agarose gel-purified PCR products (*27*) were employed directly or used as template for secondary PCR amplification under identical conditions in a total volume of 250 μL. All constructs were completely sequenced via primer walking (*27*) (DyeDeoxy Terminator Cycle Sequencing; Applied Biosystems). Unless otherwise stated, all other biochemical reagents were obtained from Sigma Chemical Co. or Aldrich Chemical Co.

Purification and Analysis of Native Limonene Synthase. Approximately 300 μg of (−)-4*S*-limonene synthase was isolated by sonic disruption of spearmint (*M. spicata*) oil gland secretory cells (*28*) and was purified to homogeneity by a protocol described in detail elsewhere (*14*, *16*). The manufacturer's protocols were followed in attempting to N-deblock the native protein with *N*-deacylase (TaKaRa Biomedical) or pyroglutamyl aminopeptidase (Sigma Chemical Co.), or using the Bio-Rad Enzymatic Deglycosylation Kit. The treated samples (∼50 μg of protein) were repurified by SDS−PAGE according to the method of Schagger and von Jagow (*29*) in preparation for electroblotting (*16*) and sequencing via Edman degradation on an Applied Biosystems 470 sequenator at the Washington State University Laboratory for Bioanalysis and Biotechnology. In preparation for ES-MS examination of the protein (courtesy of David King, University of California, Berkeley), a 150 μg sample of the limonene synthase was purified by FPLC (Pharmacia) on Mono Q and hydroxylapatite (see below) and subjected to repeated concentration and buffer exchange using a Centriprep centrifugal concentrator (Amicon) to reduce the volume and eliminate glycerol and buffer salts. Residual salts were removed by reversed-phase (C_4) HPLC immediately before MS analysis of the apparently homogeneous protein (by SDS−PAGE and HPLC).

cDNA Expression in E. coli from pET and pGEX Vectors. The coding region of the (−)-4*S*-limonene synthase cDNA clone pLC 5.2 (*16*) was amplified by PCR using *Taq* polymerase and the primers LCPCR1 (5′-GGGGGGTACCCATATGGCTCTCAAAGTGTTAAG-3′) and LCPCR2 (5′-GAGAGGATCCATGACAAAAATATATG-3′), creating a 5′-*Nde*I site at the initiation codon of the preprotein and a 3′-*Bam*HI site distal to the stop codon. The PCR product was digested with the indicated restriction enzymes, purified by ultrafiltration, and then ligated into the *Nde*I/*Bam*HI-digested pET-14b (His·Tag) expression vector (Novagen) to yield pETLC13-2. For expression from pGEX, the approximately 2.2 kb *Bam*HI/*Xho*I cDNA insert of pLC 5.2 (*16*) was subcloned into *Bam*HI/*Xho*I-digested pGEX-4T-2 (Pharmacia Biotech), resulting in plasmid pGEXLCX4-2.

Both pETLC13-2 and pGEXLCX4-2 were transformed into *E. coli* BL21(DE3)pLysS cells which were grown to $A_{600} = 0.5$ with constant shaking at 37 °C in LB medium (*27*) supplemented with 100 μg of ampicillin/mL. Cultures were then induced by addition of from 0.1 to 1.0 mM isopropyl 1-thio-β-D-galactopyranoside and grown for another 6−12 h at temperatures ranging from 20 to 37 °C. Cells were harvested by centrifugation (2000*g*, 10 min), resuspended in assay buffer (MOPSO at pH 7.0, containing $MgCl_2$ and DTT as before; 10 mL per 50 mL culture), and frozen at −20 °C. Following thawing and cell disruption by brief sonication (Braun-Sonic 2000 with microprobe at maximum power for 15 s at 0−4 °C), the homogenate was cleared by centrifugation (30000*g*, 10 min), and an aliquot of the supernatant was assayed for limonene synthase activity as described (*14*).

Inclusion bodies in the pelleted fraction were resuspended and washed in 25 mM MOPSO buffer (pH 7.0) containing 10% glycerol, 1 mM DTT, and 2 M urea or guanidine·HCl. After centrifugation at 30000*g* for 30 min, the pellet was dissolved in the same buffer containing 8 M urea or 6 M guanidine·HCl and the suspension allowed to stir at 0−4 °C or at room temperature overnight, before centrifugation (30000*g*, 30 min) and extensive dialysis of the supernatant against assay buffer containing an assortment of detergents, polyols, and cyclodextrins to assist in refolding (*30*, *31*). Following assay, both the initial soluble fraction and the material solubilized from inclusion bodies were separately purified by affinity chromatography of the respective fusion preproteins according to the manufacturer's instructions; from pET, the $(His)_6$·tagged fusion preprotein was purified on His·Bind (Ni^{2+}- or Co^{2+}-immobilized) resin (Novagen) or Talon metal affinity resin (CLONTECH), and from pGEX, the glutathione-*S*-transferase·tagged fusion preprotein was purified on glutathione−Sepharose-4B (Pharmacia Biotech). Samples of the affinity-purified preprotein were taken before and after cleavage of the fusion tag with thrombin (according to the Novagen and Pharmacia Biotech protocols) for enzyme assay, and for SDS−PAGE and immunoblotting.

Preparation of cDNA Truncations and Expression in E. coli. The spearmint limonene synthase was subcloned from the pETLC13-2 expression plasmid directly into the same restriction sites (*Nde*I and *Bam*HI) of the pSBETa expression vector. pSBETa (*32*) is a kanamycin-selectable pACYC177-based vector which carries the pET-3a-derived cloning and T7 expression region (646 bp *Eco*RI−*Bgl*I fragment), the p15a origin of replication, and an insert that encodes the low-abundance *E. coli* $tRNA_{arg^4}$ (*arg*U gene) for translation of the rare triplets AGA and AGG coding for arginine. Of the 36 arginine residues of limonene synthase, 23 (nearly 4% of the sequence) are encoded by AGA or AGG, and 17 of these rare *E. coli* codons are clustered between R118 and R338 (*16*). When pSBETa is transformed into *E. coli* BL21-(DE3) cells bearing pLysS (which also carries the p15a origin of replication, as well as chloramphenicol resistance), the plasmids recombine to form a 9 kbp plasmid carrying resistance to both antibiotics (data not shown). Compared to pETLC13-2, this large plasmid, formed in vivo from

pSBETaLC-6 and pLysS, possessed greater stability and afforded higher level expression of the preprotein. This plasmid also eliminated the problem of premature translational termination at the difficult R300WWR303 quartet of limonene synthase to yield a 35 kDa, nonfunctional peptide product (verified by immunoblotting). Therefore, a series of N-terminal truncations of the limonene synthase preprotein was constructed in pSBETaLC-6. Primers were synthesized containing an 8 nt 5′-spacer (including a *Kpn*I restriction site) overlapping an *Nde*I restriction site (CATATG) encoding the new start codon, and an additional 14−23 nt identical to the limonene synthase DNA at the site of truncation. The following primers were used for constructs: pSBETaLC-(S89)3, pSBETaLC(L76)4, pSBETaLC(Q63)5, pSBETaLC-(E57)6, pSBETaLC(S60)7, pSBETaLC(R58)8, pSBETaLC-(R58P59)8P, and pSBETaLC(R59)9, respectively: LCPCR3, 5′-GGGGGGTACCCATATGTCTGAGCTGGTCACTTTGG-3′; LCPCR4, 5′-CCCCCCTACCCATATGCTTCTCAGT-GACTATAAGG-3′; LCPCR5, 5′-GGGGGTACCATATG-CAACTCACTACTGAAAG-3′; LCPCR6, 5′-GGGGGTAC-CATATGGAAAGACGATCCGG-3′; LCPCR7, 5′-GGGG-GTACCATATGTCCGGAAACTACAACCC-3′; LCPC-R8, 5′-GGGGGTACCATATGAGACGATCCGGAAAC-3′; LCPCR8P, 5′-GGGGGTACCATATGAGACCATCCGGA-AACTACAACCC-3′; and LCPCR9, 5′-GGGGGTACCAT-ATGCGATCCGGAAACTACAACCC-3′. *Taq* DNA polymerase-based PCR was then carried out with the pETLC13-2 plasmid template using the specific primer for the truncation and a second primer (T7 terminator, Novagen) localized downstream of the coding region and of the *Bam*HI cloning site. The resulting product, consisting of the entire coding region, was then digested with *Nde*I and *Bam*HI and ligated into pSBETa. This method was used for constructs pSBE-TaLC(S89)3, pSBETaLC(L76)4, pSBETaLC(Q53)5, and pSBETaLC(E57)6 encoding, respectively, the protein truncations beginning at amino acids S89, L76, Q53, and E57. For the remaining truncations and substitutions, *Pfu* DNA polymerase-based PCR was carried out with the pLC5.2 limonene synthase target clone (*16*) using the same design of forward primers for the truncated 5′-end but, for the reverse primer, using internal limonene synthase primers (W4A or W4AA) located at nucleotides 944−928 and 950−927, respectively. The resulting product, consisting of approximately the first third of the truncated limonene synthase coding region, was then excised with *Nde*I and *Sac*I (the latter site occurring at nucleotide 912 of the limonene synthase cDNA) and cloned into the same sites in the pSBETaLC-6 plasmid, thus replacing the full-length 5′-moiety of limonene synthase with an appropriately truncated construct. By this means, the portion of the limonene synthase gene copied during PCR was reduced, thus minimizing the possibility of misincorporation of nucleotides during the reaction. pSBETaLC(R58A59)8A was generated by QuikChange Site-Directed Mutagenesis (Stratagene kit) using standard kit protocols with pSBETaLC(R58)8 as template and mutagenic primers LCPCR8AF (5′-GGAGATA-TACATTATGAGAGCATCCGGAAACTACAACC-3′) and LCPCR8AR (5′-GGTTGTAGTTTCCGGATGCTCTCAT-AATGTATATCTCC-3′).

All constructs were sequenced across the restriction sites and through the region(s) generated by PCR to ensure fidelity of the construction. Plasmid nomenclature is based upon the following scheme: vector/enzyme (amino acid beginning the truncation and any substituted residue)/primer utilized. Thus, pSBETaLC(R58)8-28b describes vector pSBETa containing the limonene cyclase (LC) gene starting at arginine 58(R58) constructed by PCR with primer LCPCR8. Multiple transformants into BL21(DE3) pLysS cells with plasmids arising from several independent ligation events were evaluated. For convenience, the corresponding expressed proteins containing the introduced methionine residue and the indicated truncation/substitution are simply referred to by the parenthetical descriptor, e.g., Q53, E57, R58P59.

The various pSBET constructs were transformed into BL21(DE3)pLysS cells (Novagen) for expression. Overnight cultures grown from single colonies were added to Fernbach flasks containing 1 L of LB medium supplemented with 50 mg of kanamycin, and the cultures were grown at 37 °C to $A_{600} = 0.5-0.7$, allowed to equilibrate to 20 °C, then induced by addition of 1 mM isopropyl 1-thio-β-D-galactopyranoside, and grown for another 12−16 h at 20 °C. Cells were harvested by centrifugation (3000*g* for 15 min) and then resuspended in 50 mL of sonication buffer [25 mM MOPSO (pH 6.8) containing 5% (v/v) glycerol, 1 mM DTT, 1 mM EDTA, and 1 mM phenylmethylsulfonyl fluoride]. Following one freeze/thaw cycle, the cells were disrupted by sonication (large probe, maximum power, 3 × 1 min) and centrifuged (30000*g* for 30 min) to remove cell debris.

The supernatant was then centrifuged at 195000*g* for 90 min, and the filtered sample (0.2 μm syringe filter, Nalgene) was loaded onto a Mono Q 10/10 column (Pharmacia FPLC) equilibrated with buffer A [25 mM MOPSO (pH 6.8) containing 5% (v/v) glycerol and 1 mM DTT]. The column was washed with buffer A until the base line stabilized, and then was eluted with a 100 mL linear gradient from 0 to 50% buffer B (buffer A plus 1 M NaCl). Limonene synthase elutes at ∼300 mM NaCl. The enzyme preparation eluted from the Mono Q column was applied directly to a ceramic hydroxylapatite column (Bio-Rad) that was equilibrated and washed with buffer A until the base line stabilized. Protein was then eluted with a 100 mL linear gradient from 0 to 30% buffer C (100 mM potassium phosphate at pH 6.8). Limonene synthase elutes at about 10 mM potassium phosphate. The course of the purification was monitored by enzyme assay, SDS−PAGE, and immunoblotting as before. By silver and Coomassie staining of SDS−PAGE gels, the truncated versions were determined to be >92% pure; due to complications arising from the presence of the plastidial transit peptide, the preprotein form of limonene synthase could not be purified to a level greater than ∼50%.

RESULTS

Monoterpene biosynthesis is compartmentalized in plastids (*33*−*36*); thus, all monoterpene synthases cloned to date are encoded as preproteins bearing an amino-terminal transit peptide for import of these nuclear gene products into plastids (leucoplasts of the oil gland cells in the present instance) where they are proteolytically processed to the mature forms (*17*, *37*). The limonene synthase of spearmint has been localized to leucoplasts by immunocytochemical methods, and this localization has been confirmed by plastidial import and processing of the in vitro translated preprotein.[1] In all of the cloned monoterpene synthases (*38*), the 50−60 amino-

terminal residues are characterized by a low degree of similarity, typical of targeting sequences (*39*), yet they all share common features of transit peptides in being rich in serine, threonine, and small hydrophobic residues but with few acidic residues (*17*, *18*, *37*). All native monoterpene synthases thus far examined (*16*, *40*−*42*) appear to be amino-terminally-blocked, preventing direct determination (by N-terminal sequencing) of the transit peptide−mature protein cleavage junction. Attempts to deblock the amino terminus of the purified, native limonene synthase by enzymatic N-deacylation, N-deglycosylation, or pyroglutamase treatment have failed to provide a protein capable of being sequenced. Electrospray ionization-mass spectrometry of the apparently homogeneous (by SDS−PAGE and HPLC) native limonene synthase indicated that this enzyme exists as a very complex heterogeneous mixture of modified species in the 65 ± 0.8 kDa size range. Confirming evidence for micro-heterogeneity (presumably arising from variations in processing) was also obtained from in vitro translation and plastidial import experiments.[1] Plastid import of the preprotein obtained by in vitro translation of the full-length cDNA in the presence of [^{35}S]methionine, [4,5-^{3}H]leucine, and [U-^{14}C]-threonine yielded, by chromatographic and electrophoretic isolation of the radiolabeled product of 65 kDa, a mixture of imprecisely processed species that afforded multiple residues upon each cycle of radiochemically based N-terminal sequencing. Thus, it was clear from these preliminary studies that detailed mechanistic and structural investigations of the recombinant limonene synthase, as a general model for terpene cyclases, would require that the expressed preprotein resemble kinetically the native form(s), or that selective truncation of the preprotein would be necessary.

Expression and Characterization of the Limonene Synthase Preprotein. To establish the kinetic behavior of the limonene synthase, full-length clone pLC5.2 (16) was initially expressed as a thrombin-cleavable, $(His)_6$·tagged (pET) or glutathione-*S*-transferase·tagged (pGEX) fusion protein to assist in purification. Expression of the preprotein in these forms, under a very broad range of induction and bacterial growth conditions, yielded the bulk of the limonene synthase (>90%) in intractable inclusion bodies, as demonstrated by SDS−PAGE and immunoblot comparison of the insoluble form to the soluble enzyme fraction (data not shown). The inclusion bodies could be solubilized with either 8 M urea or 6 M guanidine·HCl, but the unfolded protein could not be efficiently refolded to a functional species under a range of refolding conditions (*30*, *31*).

Efficient purification both of the initially soluble recombinant protein and of that solubilized from the inclusion bodies, either by separation of the $(His)_6$·tagged form (from pET) on the immobilized metal ion (Ni^{2+} or Co^{2+}) column or by separation of the glutathione-*S*-transferase-fused form (from pGEX) on the glutathione−Sepharose-4B column, proved to be difficult as less than 30% of the applied limonene synthase fusion protein could be bound to the affinity matrix and selectively eluted. Moreover, the fused preprotein that was purified by either approach always coeluted from the affinity matrix with a set of *E. coli* proteins with sizes of 30, 45, and 75 kDa. Since control experiments indicated that these bacterial proteins did not bind to the affinity matrixes in the absence of limonene synthase, their copurification with the target enzyme was attributed to the tight binding of these putative *E. coli* chaperones to the limonene synthase preprotein, most likely due to the presence of the transit peptide which would be expected to be associated with chaperones in planta (*39*). In addition to the complications imposed by the apparent binding of host chaperones, a significant fraction (up to 50%) of the limonene synthase preprotein expressed from pET or pGEX vectors was truncated to 35 kDa as shown by SDS−PAGE and immunoblotting (data not shown). The latter was attributed to translation termination at the difficult R300WWR303 element, likely due to both rare arginine codon usage and low abundance of tryptophan tRNA. These limitations in the expression of the affinity-tagged fusion proteins necessitated further purification of the preprotein by anion-exchange and hydroxylapatite chromatography, after thrombin cleavage of the affinity tag, before sufficiently pure material (~40% by SDS−PAGE) could be obtained to estimate kinetic properties. The limonene synthase preprotein so obtained, from either pET or pGEX expression system, yielded a K_m value for geranyl diphosphate of about 16 μM and a k_{cat} value of nearly 0.020 s^{-1}; these compare to K_m and k_{cat} values of 6.7 μM and 0.024 s^{-1}, respectively, recently redetermined for the purified, native form(s) under identical conditions.[3]

In an attempt to eliminate the truncated limonene synthase species, and to investigate in greater detail the limitations imposed by *E. coli* chaperone binding in the purification, the full-length limonene synthase cDNA was subcloned from pET into pSBETa, a pAC-based vector that additionally encodes a tRNA for rare arginine codon usage in *E. coli* which is common in higher plants (*32*). The preprotein so expressed (~5% of total *E. coli* protein) was still largely produced as intractable inclusion bodies (~50%) under optimized conditions, but no truncated species were present in either the inclusion bodies or the soluble form of the enzyme, as determined by SDS−PAGE and immunoblotting. The association of *E. coli* chaperones with the soluble preprotein was still apparent on purification, however, indicating that this complication was not due to the presence of the fusion tags in the previously expressed forms. Nevertheless, the combination of anion-exchange and hydroxylapatite chromatography allowed partial purification of the unmodified preprotein (to about 50% purity with a 5% yield), which was used to determine a K_m value of 14.9 μM and a k_{cat} value of 0.020 s^{-1}. Thus, it was evident that the limonene synthase preprotein was also kinetically compromised relative to the native enzyme(s) and thus of limited utility for detailed mechanistic and structural investigation. Also, the presence of a sizable, and largely unstructured, amino-terminal transit peptide (*43*) would likely make this form unsuitable for X-ray crystallographic study.

Expression and Characterization of Limonene Synthase N-Terminal Truncations. Given the limitations in the properties, and difficulties in the purification, of the limonene synthase preprotein, and the inability to directly determine the transit peptide−mature protein junction, it was necessary to construct a series of N-terminal truncations to provide a 'pseudomature' form of the enzyme that kinetically resembled the native species. The initial two truncations, pSBETaLC(L76)4 and pSBETaLC (S89)3, were located near

[3] This k_{cat} value corrects a systematic error in a prior estimate (*14*).

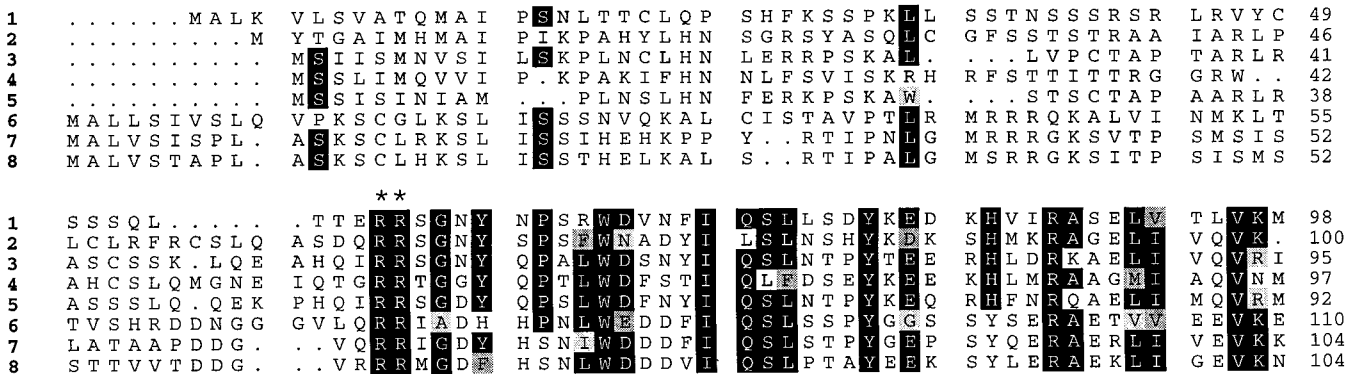

FIGURE 1: Comparison of amino-terminal sequences surrounding the tandem arginines of cloned monoterpene synthases. The sequences indicated are **1**, (−)-limonene synthase from spearmint (*16*); **2**, (−)-limonene synthase from *Perilla frutescens* (44); **3**, (+)-bornyl diphosphate synthase; **4**, 1,8-cineole synthase; **5**, (+)-sabinene synthase from common sage (45); **6**, (−)-limonene synthase; **7**, mycene synthase; and **8**, (−)-pinene synthase from grand fir (46). The tandem arginines are marked by asterisks. Residues boxed in black are identical for at least five of the eight compared sequences. The alignment was created with the GCG *PILEUP* program.

potential cleavage sites according to the predictive algorithms of Gavel and von Heijne (*18*) and von Heijne and associates (*17*), respectively, viz., a hydrophobic moment and predicted β-sheet structure in a region enriched in arginine and depleted of leucine immediately upstream of the cleavage site. With these truncations, however, no significant activity (<0.1% of the preprotein) was detected, and the resulting expressed proteins were visibly shorter than the mature, native proteins on SDS−PAGE.

Therefore, a series of trunctions was made around the tandem arginine residues at positions 58 and 59 of the preprotein. This motif is conserved in the deduced sequences of all of the monoterpene synthases cloned to date (*44*−*46*) (Figure 1), and the identity scores for the alignments upstream (23−28%) and downstream (52−70%) of this element differ markedly for the enzymes of angiosperm origin, apparently defining the most amino-terminal region of obvious homology and thereby suggesting a possible cleavage site. This comparison is most obvious in the sequence alignments (Figure 1, **1** and **2**) of (−)-4*S*-limonene synthase from spearmint (*16*) and from *Perilla frutescens* (*44*) (24% identity upstream and 70% identity downstream of the RR element for these closely related members of the mint family), and it serves to confirm the great sequence variation in transit peptides and cleavage sites, even for the same synthase from allied species. Truncations surrounding the double arginines were constructed in the pSBET vector, and the corresponding proteins were purified for kinetic evaluation. It is notable that all of the limonene synthase truncations were readily purified (to >92% in >40% yield) by the combination of anion-exchange and hydroxylapatite chromatography, since each was expressed as a soluble enzyme (at ∼20% of total *E. coli* soluble protein) which was not apparently associated with the bacterial chaperones. These observations indicate that the transit peptide of the limonene synthase preprotein is largely responsible for promoting the formation of inclusion bodies with this form of the enzyme, and that the transit peptide is also the target for the binding of bacterial chaperones.

Comparison of K_m and k_{cat} values of the truncations to those values of the mature, native enzyme mixture (Table 1) suggests a likely cleavage site in the preprotein, allowing the preparation of a highly active 'pseudomature' limonene synthase in the appropriate molecular mass range (∼65 kDa)

Table 1: Kinetic Constants for the Native Form, Full-Length Preprotein, and Truncated Versions of Limonene Synthase[a]

	geranyl diphosphate		3S-linalyl diphosphate	
enzyme	K_m (μM)	k_{cat} (s^{-1})	K_m (μM)	k_{cat} (s^{-1})
native	6.7	0.024	22.2	0.063
preprotein	14.9	0.020		
Q53	8.6	0.036		
E57	6.0	0.034		
R58	12.6	0.037	35.3	0.082
R59	29.9	<0.0004	48.2	0.105
R58P59	32.4	<0.0004		
R58A59	27.5	<0.0004		
S60	18.8	<0.0004		
L76	>100	<0.0002		
S89	>100	<0.0002	61.3	0.017

[a] No entry indicates not determined. Kinetic constants are averaged data sets of triplicate analyses with SE less than 10% of the indicated value.

by truncation immediately upstream of the tandem R58R59 residues. That none of the active truncations has the same kinetic behavior as the native form may be attributed to the facts that the native enzyme represents a heterogeneous mixture of species with uncertain N-terminal modification-(s) and that the recombinant proteins are expressed with formylmethionine at the amino terminus. In a similar sense, it is not possible to determine whether the difference in K_m values between the E57 and R58 truncations is due to the absence of the glutamate residue at position 57 of the latter or to the substitution of methionine. Given that most of the monoterpene synthases thus far defined contain an upstream acidic residue, either glutamate or aspartate, within a few amino acids of the RR motif (Figure 1), and that acidic residues are infrequent in transit peptides (*18*), it seems most reasonable to assume that cleavage would occur amino-terminal to the acidic residue and that, in the present instance, E57 would be included in the mature protein where it may contribute to substrate binding.

The olefin mixtures generated by the native enzyme, preprotein, and truncations were examined by GC-MS at both low and high substrate concentration and shown to be identical [94% (−)-limonene, with equivalent, minor amounts of myrcene, (−)-α-pinene, and (−)-β-pinene] despite the differing kinetic constants between these enzyme forms. This observed fidelity suggests that truncation influences the interaction with the diphosphate moiety of the substrate, the

primary binding determinant (*47*, *48*), and alters the rate-limiting ionization step of the reaction (*9*, *49*), without appreciably altering the binding site to modify reacting conformations of the olefinic substrate chain that direct product outcome.

Removal of both arginine residues (S60) or merely the first (R59) results in severely decreased k_{cat} values to less than 1% of the native enzyme (Table 1). Moreover, substitution of the second arginine by proline (i.e., R58P59), or by a small hydrophobic residue (e.g., R58A59), as found in several cytosolic sesquiterpene synthases or plastidial diterpene synthases (*50*−*56*), also reduced activity to a negligible level (Table 1). These observations suggest that the tandem arginines, a feature specific to the monoterpene synthases, are of functional significance in this class of terpenoid synthase.

DISCUSSION

Truncation amino terminal to the tandem pair of arginine residues of the limonene synthase preprotein provides 'pseudomature' forms of this monoterpene cyclase that are kinetically more efficient than the heterogeneous native enzyme(s) from spearmint oil glands. Moreover, the truncated recombinant enzymes expressed from pSBET constructs are more readily purified than the expressed preprotein, since they neither form inclusion bodies nor serve as a target for bacterial chaperones which bind to and copurify with the preprotein. Since all monoterpene synthases cloned to date possess a tandem pair of arginines at the same relative location (50−70 residues from the starting methionine; see Figure 1), it appears that this motif is close to and downstream of the targeting peptide cleavage site for these plastid-directed enzymes.

The profound influence of truncation beyond R58 cannot be due simply to the length of this N-terminal extension, since both R58P59 and R58A59 variants are inactive. The effect must relate to the tandem arginines themselves which represent a unique sequence motif of all the monoterpene synthases from both angiosperms and gymnosperms. This motif is replaced by RP, RA, or related elements in the sesquiterpene and diterpene synthases of plant origin. While the mechanism of monoterpene cyclization is very similar to that of sesquiterpene and diterpene cyclization, the monoterpene synthases are unique among the terpene synthases in an absolute requirement for a preliminary isomerization step to convert the geranyl diphosphate substrate to enzyme-bound linalyl diphosphate prior to cyclization (Scheme 1) (*8*, *9*, *57*). This novel mechanistic feature may be related to the required tandem RR motif.

The crystal structure of the sesquiterpene cyclase of plant origin, epi-aristolochene synthase from tobacco, has been solved, and homology modeling studies indicate limonene synthase to be very similar to epi-aristolochene synthase in overall three-dimensional structure (*58*). The amino-terminal domain (residues 36−230) of epi-aristolochene synthase aligns structurally with several glycosyl hydrolases and has been suggested to play a role in the interaction with other macromolecular structures (*58*); the carboxy-terminal domain, which contains the active site, is topologically similar to the mechanistically related prenyltransferase farnesyl diphosphate synthase (*59*). On substrate binding by epi-aristolochene synthase, the previously unstructured N-terminus (residues 17−35, corresponding to residues 60−78 of limonene synthase), that is located very near the surface of the active site, becomes ordered and translates to extend the outer wall of the catalytic pocket, in part via hydrogen bonding between R266 (R317 in limonene synthase) and S21 (S60 or S66 of limonene synthase) of the N-terminal segment (*58*). Upon substrate ionization, the negative charge of the diphosphate anion is offset by interaction with Mg^{2+} ions, as well as with R264 and R441 (R315 and R493 of limonene synthase), and directed away from the hydrophobic pocket where the carbocation undergoes subsequent reaction to the terminal olefin product.

In the case of the monoterpene cyclase, placement of the tandem arginines at the outer surface of the active site upon substrate binding and ionization may serve, through electrostatic interactions with the newly formed diphosphate, to prevent premature loss of the diphosphate or regeneration of the substrate by positioning of the diphosphate near the C3 cationic center of the olefinic substrate chain. This structural arrangement would promote isomerization to the essential linalyl diphosphate intermediate by recapture of the diphosphate at the C3 carbocation center (Scheme 1). Such a role for the tandem arginines at the periphery of the active site pocket is consistent with the inactivation of limonene synthase by arginine-directed reagents in a manner that is not prevented by prior substrate addition (*60*). Thus, although catalytically important methionine, cysteine, histidine, and arginine residues appear, by homology modeling, to lie within the catalytic pocket of limonene synthase, only arginine is not protected against specific alkylating agents by substrate binding (*22*, *60*). In strong support of the suggestion that the role of the N-terminal arginine pair is to assist in the isomerization step of the reaction sequence, the R59 truncated enzyme, which is incapable of utilizing the normal substrate geranyl diphosphate, is able to convert the isomerized intermediate 3*S*-linalyl diphosphate to (−)-limonene with respectable kinetics (K_m ∼48.2 μM and k_{cat} ∼0.105 s^{-1}, compared to K_m ∼22.2 μM and k_{cat} ∼0.063^{-1} for the native enzyme identically determined). Even truncated version S89, representing cleavage well into the N-terminal "glycosyl hydrolase" domain of the limonene synthase, although completely incapable of carrying out the coupled isomerization and cyclization of the native geranyl substrate (Table 1) is able to cyclize exogenous 3*S*-linalyl diphosphate (K_m ∼61.3 μM; k_{cat} ∼0.017 s^{-1}). This observation suggests that a glycosyl hydrolase may have been recruited early in the course of evolution of the enzyme class (*38*) to conduct the isomerization component of the now coupled isomerization−cyclization reaction sequence catalyzed by the monoterpene synthases. Definition of the precise role of the arginine pair and of additional residues of the amino-terminal domain will require determination of the three-dimensional structure of limonene synthase; this work is in progress.

ACKNOWLEDGMENT

We thank David King for the mass spectrometric analyses, E. Stauber, G. Munske, and D. Pouchnik for amino acid and nucleotide sequencing, and Joyce Tamura for preparation of the manuscript.

REFERENCES

1. Connolly, J. D., and Hill, R. A. (1991) *Dictionary of Terpenoids*, Chapman and Hall, London.
2. Harborne, J. B. (1991) in *Ecological Chemistry and Biochemistry of Plant Terpenoids* (Harborne, J. B., and Tomas-Barberan, R. A., Eds.) pp 399−426, Clarendon Press, Oxford.
3. Ogura, K., and Koyama, T. (1997) in *Dynamic Aspects of Natural Products Chemistry* (Ogura, K., and Sankawa, U., Eds.) pp 1−23, Kodansha, Tokyo.
4. Chappell, J. (1995) *Annu. Rev. Plant Physiol. Mol. Biol. 46*, 521−547.
5. McGarvey, D., and Croteau, R. (1995) *Plant Cell 7*, 1015−1026.
6. Cane, D. E. (1998) *Comprehensive Natural Products Chemistry: Isoprenoids*, Vol. 2, Elsevier Science, Oxford.
7. Lesburg, C. A., Zhai, G., Cane, D. E., and Christianson, D. W. (1997) *Science 277*, 1820−1824.
8. Wise, M. L., and Croteau, R. (1998) in *Comprehensive Natural Products Chemistry: Isoprenoids* (Cane, D. E., Ed.) Vol. 2, Elsevier Science, Oxford (in press).
9. Rajaonarivony, J. I. M., Gershenzon, J., and Croteau, R. (1992) *Arch. Biochem. Biophys. 296*, 49−57.
10. Croteau, R., and Satterwhite, D. M. (1989) *J. Biol. Chem. 264*, 15309−15315.
11. Cori, O., Chayet, L., Perez, L. M., Bunton, C. A., and Cori, M. (1986) *J. Org. Chem. 51*, 1310−1317.
12. Cramer, F., and Rittersdorf, W. (1967) *Tetrahedron 23*, 3015−3022.
13. Haley, R. C., Miller, J. A., and Wood, H. C. S. (1969) *J. Chem. Soc. (C)*, 264−268.
14. Alonso, W. R., Rajaonarivony, J. I. M., Gershenzon, J., and Croteau, R. (1992) *J. Biol. Chem. 267*, 7582−7587.
15. Crowell, P. L., and Gould, M. N. (1994) *CRC Crit. Rev. Oncogenesis 5*, 1−22.
16. Colby, S. M., Alonso, W. R., Katahira, E. J., McGarvey, D. J., and Croteau, R. (1993) *J. Biol. Chem. 268*, 23016−23024.
17. von Heijne, G., Steppuhn, J., and Herrmann, R. G. (1989) *Eur. J. Biochem. 180*, 535−545.
18. Gavel, Y., and von Heijne, G. (1990) *FEBS Lett. 261*, 455−458.
19. Croteau, R., Alonso, W. R., Koepp, A. E., and Johnson, M. A. (1994) *Arch. Biochem. Biophys. 309*, 184−192.
20. Satterwhite, D. M., Wheeler, C. J., and Croteau, R. (1985) *J. Biol. Chem. 260*, 13901−13908.
21. Croteau, R., Felton, M., Karp, F., and Kjonaas, R. (1981) *Plant Physiol. 67*, 820−824.
22. Rajaonarivony, J. I. M., Gershenzon, J., Miyazaki, J., and Croteau, R. (1992) *Arch. Biochem. Biophys. 299*, 77−82.
23. Bradford, M. M. (1976) *Anal. Biochem. 72*, 248−254.
24. Laemmli, U. K. (1970) *Nature (London) 227*, 680−685.
25. Blum, H., Beier, H., and Gross, H. J. (1987) *Electrophoresis 8*, 93−99.
26. Alonso, W. R., Crock, J. E., and Croteau, R. (1993) *Arch. Biochem. Biophys. 301*, 58−63.
27. Sambrook, J., Fritsch, E. F., and Maniatis, T. (1989) *Molecular Cloning: A Laboratory Manual*, 2nd ed.; Cold Spring Harbor Laboratory, Plainview, NY.
28. Gershenzon, J., McCaskill, D., Rajaonarivony, J. I. M., Mihaliak, C., Karp, F., and Croteau, R. (1992) *Anal. Biochem. 200*, 130−138.
29. Schagger, H., and von Jagow, G. (1987) *Anal. Biochem. 166*, 368−378.
30. Rozema, D., and Gellman, S. H. (1995) *J. Am. Chem. Soc. 117*, 2373−2374.
31. Zardeneta, G., and Horowitz, P. M. (1994) *Anal. Biochem. 223*, 1−6.
32. Schenk, P. M., Baumann, S., Mattes, R., and Steinbiss, H.-H. (1995) *BioTechniques 19*, 196−200.
33. Gleizes, M., Pauly, G., Carde, J.-P., Marpeau, A., and Bernard-Dagan, C. (1983) *Planta 159*, 373−381.
34. Mettal, U., Boland, W., Beyer, P., and Kleinig, H. (1988) *Eur. J. Biochem. 170*, 613−616.
35. Perez, L. M., Pauly, G., Carde, J.-P., Belingheri, L., and Gleizes, M. (1990) *Plant Physiol. Biochem. 28*, 221−229.
36. Soler, E., Feron, G., Clastre, M., Dargent, R., Gleizes, M., and Ambid, C. (1992) *Planta 187*, 171−175.
37. Keegstra, K., Olsen, J. J., and Theg, S. M. (1989) *Annu. Rev. Plant Physiol. Mol. Biol. 40*, 471−501.
38. Bohlmann, J., Meyer-Gauen, G., and Croteau, R. (1998) *Proc. Natl. Acad. Sci. U.S.A. 95*, 4126−4133.
39. Kouranov, A., and Schnell, D. J. (1996) *J. Biol. Chem. 271*, 31009−31012.
40. Lewinsohn, E., Gijzen, M., and Croteau, R. (1992) *Arch. Biochem. Biophys. 293*, 167−173.
41. McGeady, P., and Croteau, R. (1995) *Arch. Biochem. Biophys. 317*, 149−155.
42. Steele, C. L., Lewinsohn, E., and Croteau, R. (1995) *Proc. Natl. Acad. Sci. U.S.A. 92*, 4164−4168.
43. Horniak, L., Pilon, M., van't Hof, R., and de Kruiff, B. (1993) *FEBS Lett. 334*, 241−246.
44. Yuba, A., Yazaki, K., Tabata, M., Honda, G., and Croteau, R. (1996) *Arch. Biochem. Biophys. 332*, 280−287.
45. Wise, M. L., Savage, T. J., Katahira, E., and Croteau, R. (1998) *J. Biol. Chem. 273*, 14891−14899.
46. Bohlmann, J., Steele, C. L., and Croteau, R. (1997) *J. Biol. Chem. 272*, 21784−21792.
47. Wheeler, C. J., and Croteau, R. (1987) *J. Biol. Chem. 262*, 8213−8219.
48. Wheeler, C. J., and Croteau, R. (1988) *Arch. Biochem. Biophys. 260*, 250−256.
49. Croteau, R. (1986) *Arch. Biochem. Biophys. 251*, 777−782.
50. Facchini, P. J., and Chappell, J. (1992) *Proc. Natl. Acad. Sci. U.S.A. 89*, 11088−11092.
51. Mau, C. J. D., and West, C. A. (1994) *Proc. Natl. Acad. Sci. U.S.A. 91*, 8497−8501.
52. Back, K., and Chappell, J. (1995) *J. Biol. Chem. 270*, 7375.
53. Chen, X.-Y., Chen, Y., Heinstein, P., and Davisson, V. J. (1995) *Arch. Biochem. Biophys. 324*, 255−266.
54. Wildung, M. R., and Croteau, R. (1996) *J. Biol. Chem. 271*, 9201−9204.
55. Crock, J. E., Wildung, M., and Croteau, R. (1997) *Proc. Natl. Acad. Sci. U.S.A. 94*, 12833−12838.
56. Steele, C. L., Crock, J. E., Bohlmann, J., and Croteau, R. (1998) *J. Biol. Chem. 273*, 2078−2089.
57. Croteau, R. (1987) *Chem. Rev. 87*, 929−954.
58. Starks, C. M., Back, K., Chappell, J., and Noel, J. P. (1997) *Science 277*, 1815−1820.
59. Tarshis, L. C., Yan, M., Poulter, C. D., and Sacchettini, J. C. (1994) *Biochemistry 33*, 10871−10877.
60. Savage, T. J., Ichii, H., Hume, S. D., Little, D. B., and Croteau, R. (1995) *Arch. Biochem. Biophys. 320*, 257−265.

BI980854K